MISSIONE 4
ISTRUZIONE RICERCA

D4.11.2: Documentation of desert dust product [B8]

Finanziato dall'Unione europea NextGenerationEU
Ministero dell'Università e della Ricerca
Italiadomani PIANO NAZIONALE DI RIPRESA E RESILIENZA

Deliverable number:	D4.11.2
Work package:	WP4 – Atmosphere
Intermediate Objective:	IO4.4
Deliverable type:	X Document, report
	☐ Websites, patent filings, videos, etc.
	☐ Other: please specify .....
Dissemination level:	X Public
	☐ Restricted
Estimated delivery (bimester):	B8
Actual delivery date:	
Author(s) (Partner-OU):	Michail Mytilinaios, Benedetto De Rosa, Serena Trippetta, Pilar Guma Claramunt, Gianluca Di Fiore, Lucia Mona (CNR-IMAA)
Reviewed by:	Giandomenico Pace (ENEA)
Note:	

IR0000032 – ITINERIS, Italian Integrated Environmental Research Infrastructures System - CUP B53C22002150006 (D.D. n. 130/2022)
Funded by EU - Next Generation EU
Mission 4 “Education and Research” - Component 2: “From research to business” -
Investment 3.1: “Fund for the realisation of an integrated system of research and innovation infrastructures”

Table of contents

Index of figures

INTRODUCTION

This document describes a product resulting from aerosol lidar measurements of interest for investigating the occurrence and relevance of desert dust outflows from Northern Africa over Italy. The product is connected to activity 4.11 concerning *atmospheric aerosol typing* and it is also linked to activity in task 8.5, where a virtual research environment making use of such product is being developed.

This document is structured in two main parts, one describing the relevance and effects of desert dust in air quality, climate variability, environmental processes and climate change, one describing how the developed desert dust product is obtained starting from the standard aerosol lidar products. An annex reports the designed format of netcdf file for accommodating such a product keeping high the level of traceability and fairness used into ACTRIS aerosol remote sensing data center.

THE IMPORTANCE OF DESERT

Atmospheric desert dust is one of the major contributors to global aerosol loading and is the dominant component of atmospheric aerosols over large areas of the Earth. Mineral dust particles, suspended in the atmosphere from arid and semi-arid regions, can remain in the atmosphere for a time ranging from some days to about a week, depending on their size, e.g. dust particles with an aerodynamic diameter lesser than 10 μm have a relatively longer lifetime in the atmosphere and can be transported downwind over long distances. Eventually, under favorable meteorological conditions large amounts of dust can be transported in the free troposphere over great distances, affecting regions hundreds to thousands of kilometers away (Schepanski et al., 2017; Yu et al., 2021; Nogueira et al., 2021).

The impact of atmospheric dust on the environment, human and animal health, and economies represents a major scientific and societal issue (WHO, 2021; UNCCD, 2022; Monteiro et al., 2022 ; Mona et al., 2023). Figure 1 represents the main processes and impacts of dust aerosols. Dust aerosols can interact with solar and thermal radiation and with clouds, affecting radiative forcing and precipitation formation and thus influencing Earth's weather and climate. Once the dust is deposited, either by wet or dry deposition, it impacts both aquatic and terrestrial ecological systems through several different biogeochemical processes; e.g., mineral dust contains micronutrients that can act as a fertilizer.

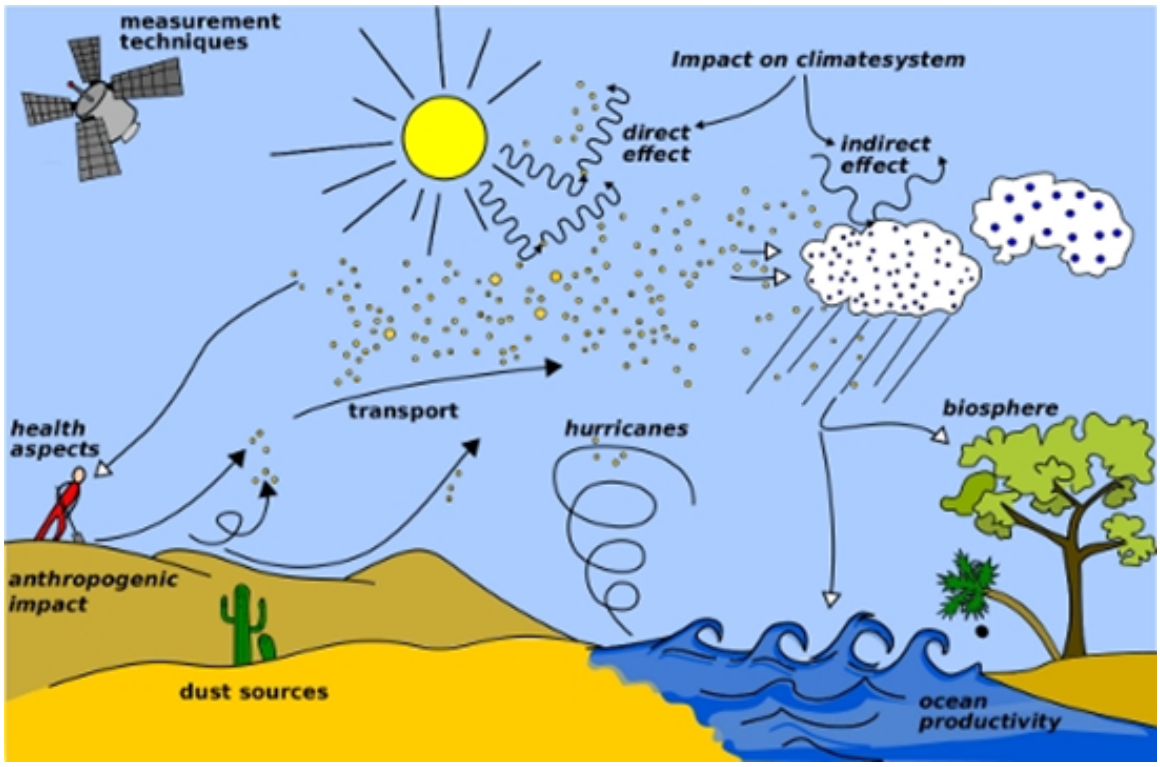

Figure 1: Atmospheric dust process and impacts on environment (https://community.wmo.int/en/sds-about)

For countries in and downwind of arid regions, airborne sand and dust has numerous implications for various socio-economic sectors, such as public health and infrastructures. High concentrations of dust in residential areas degrade air quality and pose a significant threat to public health. Typical pathological responses to dust particles are respiratory problems and cardio-vascular diseases (Gupta et al., 2012; Vergadi et al., 2022). Moreover, the atmospheric transport of dust particles may also enhance the risk of bacterial infections such as meningitis.

Extreme dust events can also cause infrastructure malfunction and significant economic losses, on sectors such as transportation, aviation and solar energy production. More specifically, during intense dusty conditions, low visibility can cause road traffic disruptions and accidents and disturbances in airport operations leading to delays and cancellations of flights. In addition, dust particles can cause mechanical damages to the aircraft, including engine erosion and corrosion. For solar energy plants, the presence of dust in the atmosphere causes attenuation of the incoming solar irradiance and a reduction of the solar panel efficiency upon deposition (soiling), leading to a significant reduction of solar energy production Cordero et al., 2018; Kennedy et al., 2021).

The Sahara Desert in north Africa and the deserts located in the Middle East are the most important dust sources of the planet and dust from these sources is frequently driven to America, Asia and Europe. Due to the proximity to the Sahara and the Arabic deserts, the Mediterranean Basin is affected by dust outbreaks throughout the year (Gkikas et al., 2013, 2016), as mineral particles originating primarily from north African and secondarily from the deserts of the Arabian Peninsula are transported towards the Mediterranean Sea under the prevalence of cyclonic systems (Fig. 2; Flaounas et al., 2015; Gkikas et al., 2015).

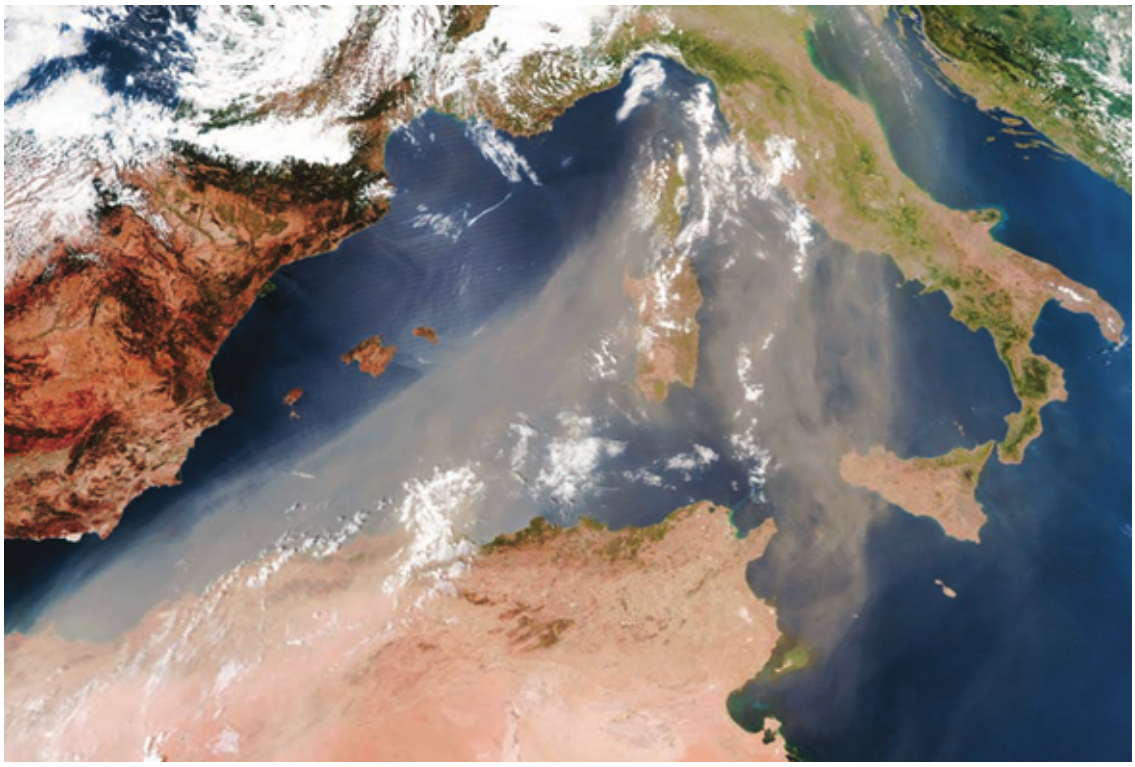

Figure 2: Terra satellite image of a huge dust plume crossing the Mediterranean Sea. This image was taken on 16 July 2003 by NASA's Moderate Resolution Imaging Spectroradiometer (MODIS). NASA/Science Photo Library.

The position of the prevailing synoptic systems is subject to an intra-annual variation, inducing a seasonal pattern of dust intrusions over the Mediterranean basin. The Central Mediterranean region and more specifically Italy, are usually affected by dust loads mainly in spring and in summer, whereas between the months of November and January the dust activity is quite weak (Pace et al., 2006; Mona et al., 2006, 2014; Meloni et al., 2007; Boselli et al., 2012; Gkikas et al., 2022). However, regardless of the time of year, high-intensity dust events have been reported across the country that persist in the free troposphere and near the surface for several days, especially in Southern Italy. Eventually, the quantity of the dust burden that arrives in Italy is capable to exert significant impacts on environment and on socio-economic sectors (Mallone et al., 2011; Barnaba et al., 2017; Di Mauro et al., 2019). It is therefore of great social and scientific interest to better understand atmospheric dust processes and study the intensity, the duration, and the variability of the dust events, in order to mitigate their unwanted impacts.

DUST EXTINCTION PROFILES

Among the various observational techniques for desert dust particles detection and characterization (see for a review Mona et al., 2023), aerosol lidar depolarization technique has the unique advantage of allowing the direct identification of desert dust particles, thanks to depolarizing signal coming from aspherical particles like desert dust ones, with a very high precision in terms of vertical distribution, because of the unique capability of lidar of providing information on the particle vertical distribution.

A detailed review of lidar capabilities for mineral dust investigation is reported in Mona et al. (2012). A key element for the investigation of mineral dust is the retrieval of the particle depolarization ratio profiles that can be achieved by using specific detection channel(s) (e.g., Sugimoto et al., 2003). After an accurate calibration of a depolarization lidar system (Freudenthaler et al., 2009), the particle linear depolarization ratio (providing information on the particle shape) allows the discrimination of

mineral dust within an atmospheric volume and the consequent derivation of the pure-dust backscatter coefficient profile (Marenco and Hogan, 2011; Ansmann et al., 2012) and, in case of Raman/ HSRL lidar systems, the dust extinction coefficient profile (Shimizu et al., 2017; Tesche et al., 2009; Yumimoto et al., 2008) and dust optical depth by the integration of the dust extinction profile.

One of the goal of ITINERIS, is to develop specific desert dust lidar datasets to be provided through the ITINERIS Hub (workpackage 2). These datasets will be implemented talking advantage of the 5 active ACTRIS/EARLINET stations in Italy, to be enlarged to other lidar stations whenever available.

EARLINET (European Aerosol Research LIdar NETwork) network is one of the ACTRIS constituting network and nowadays consists of more than 30 operating lidar stations across Europe, providing daytime and night-time measurements of aerosol optical properties, twice per week on average, since 2000. The main products of an EARLINET lidar system are the aerosol backscatter and extinction coefficient profiles as well as the intensive properties that derive from them, namely the Ångström exponent (AE) and the lidar ratio (LR). These latter 2 parameters can provide very useful information for the identification of dust layers in the atmosphere, along with back-trajectory analysis. Anyhow, since 2012, many EARLINET stations started performing depolarization ratio measurements, which are extremely precious for distinguishing non-spherical particles, such as desert dust, from other aerosol types, using a methodology that separates the dust component from the total aerosol profile (Tesche et al., 2009).

In particular, our desert dust products will be *Dust Backscatter Coefficient* (DBC) and *Dust Extinction Coefficient* (DEC), that are higher level lidar products which can be obtained by the typical EARLINET's products of Particle Backscatter Coefficient (PBC) and Particle Depolarization Ratio (PDR) profiles. The retrieval is based on the separation of the dust component from the total aerosol PBC profile, using the PDR for distinguishing non-spherical particles, as mineral dust, from other aerosols, following the methodology introduced by Tesche et al. (2009). In order to assure the quality of the final products, only quality assured (Level 2.0) PBC and PDR data according to the latest EARLINET Quality Check procedure will be used (QC 3.0; https://www.earlinet.org/index.php?id=293), downloaded by the EARLINET database. As most lidar systems in the network perform PDR measurements at 532 nm, we only use products at this wavelength; however, the process for retrieving the dust profiles presented here is similar for the 355 nm as well.

Before the DBC retrieval process, an additional check is made on the PBC and PDR to verify that from a technical and physical point of view there are no values that can bias the calculation of DBC. More specifically, as shown in the flowchart of Fig. 3, the two profiles PBC(z) and PDR(z) and their errors, δPBC(z) and δPDR(z) respectively, are individually vertically inspected and for each altitude bin (z) the following controls are performed:

1 - the adopted separation methodology requires that all four variables are available; even if only one of them is missing (= NaN), the calculation of the DBC is impossible.

2 - data are considered only if the relative uncertainty (error-to-signal ratio) does not exceed a maximum value of 50%, otherwise data are not considered reliable to be used in the DBC calculation.

3 - the presence of aerosols in the atmosphere is checked. If PBC(z) is lower than a minimum aerosol content limit, it is assumed that the aerosol load at that altitude is very small, and so no dust particles can be identified , i.e., DBC(z) = 0. According to the EARLINET QC procedure this threshold value is set at PBCdect = 5·10-7 m-1 sr-1.

4 - Lastly, the bins where PBC is contaminated by cirrus clouds and where the relative uncertainty of PDR is ≥ 50 % are excluded.

Data that passed all these four controls are used to calculate DBC and its error δDBC. In this process measurements of PDR are used to categorize the shape of the particles into three different types: spherical, mixed type and non-spherical. More specifically, if the value of PDR is less than 0.05, the all particles are considered spherical (i.e., there is no dust at the given height z), whereas if it is greater than 0.31, non-spherical particles (mineral dust) dominate. For intermediate values, a separation equation is applied to calculate the percentage of non-spherical particles in the total aerosols (Tesche et al., 2009). In detail, DBC and δDBC are calculated as follows:

$$\text{If} \quad PDR(z) \le PDR_{nd} \longrightarrow \begin{cases} DBC(z) = 0 \\ \delta DBC(z) = 0 \end{cases}$$

If

$$PDR_{nd} < PDR(z) < PDR_{d} \longrightarrow \begin{cases} DBC(z) = PBC(z)\dfrac{(PDR(z) - PDR_{nd})\cdot(1 + PDR_{d})}{(PDR_{d} - PDR_{nd})\cdot(1 + PDR(z))} \\ \delta DBC(z) = \sqrt{\left(\delta PBC(z)\cdot\dfrac{\partial DBC(z)}{\partial PBC(z)}\right)^{2} + \left(\delta PDR(z)\cdot\dfrac{\partial DBC(z)}{\partial PDR(z)}\right)^{2}} \end{cases}$$

$$\text{If} \quad PDR(z) \ge PDR_{d} \longrightarrow \begin{cases} DBC(z) = PBC(z) \\ \delta DBC(z) = \delta PBC(z) \end{cases}$$

where PDR_{nd} = 0.05 and PDR_{d} = 0.31 are the threshold values for non-dust and dust particles respectively. The error δDBC is computed by applying the general formula of error propagation to the separation equation.

Finally, the DEC is estimated by multiplying the DBC by a typical lidar ratio (LR) at 532 nm equal to 55 sr, representative of desert dust particles detected over Europe, mainly originating in northern Africa (Papagiannopoulos et al., 2018).

$$DEC(z) = LR(\lambda)\cdot DBC(z)$$

$$\delta DEC(z) = LR(\lambda)\cdot \delta DBC(z)$$

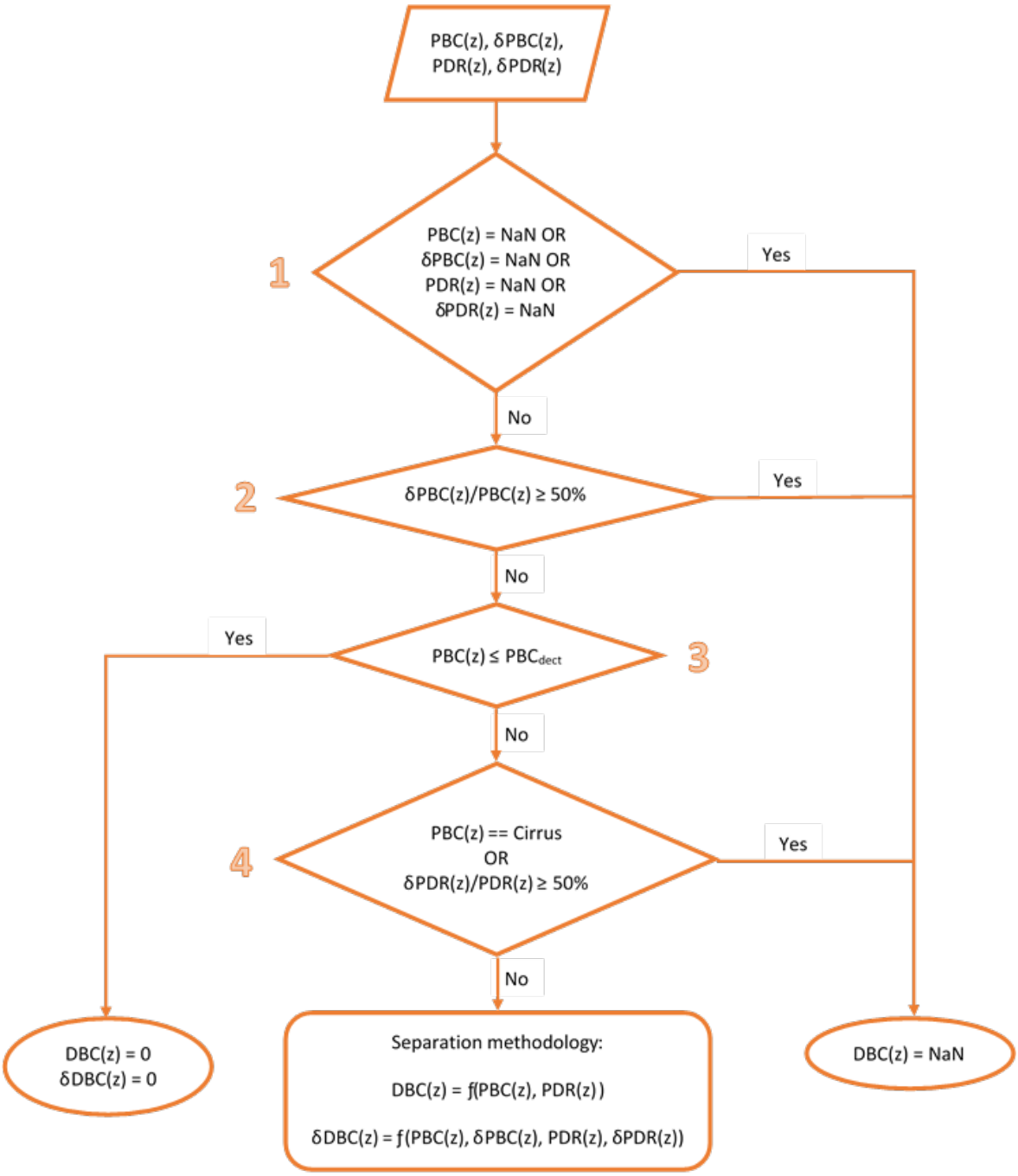

Figure 3: The profiles of PBC, PDR and their errors are scanned and the values that do not pass the four controls are excluded from the DBC calculation process.

Together to the statistical errors, the method has obviously some uncertainties due to the made assumptions. The accuracy of such dust backscatter and extinction calculation was checked by Tesche et al., 2009 through a sensitivity study, showing that relative errors for the dust components are about 20% and 25% for backscatter and extinction, respectively.

Figure 4 shows an example of how we arrive at the calculation of DEC according to the procedure described above, and concerns an actual measurement made at Potenza station.

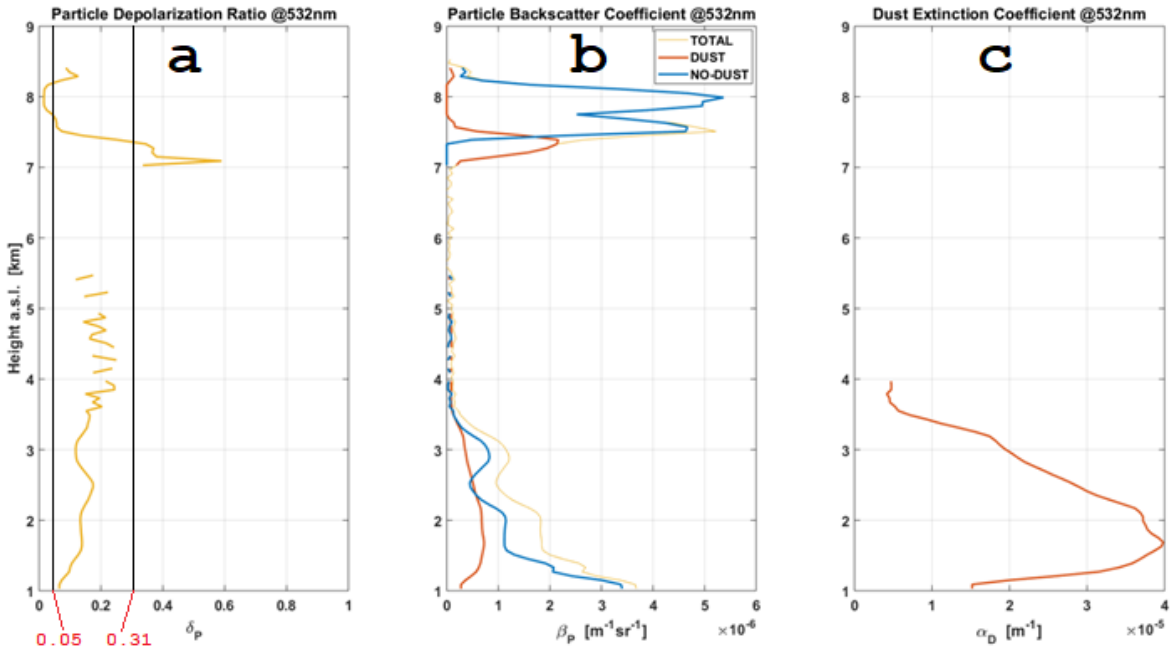

Figure 4: Retrieval of the DEC profile (c) from measurements of PDR (a) and PBC (b) made at the EARLINET station of Potenza, on May 7th 2015, between 20:46 and 22:16 UTC.

The total PBC is divided into components dust and non-dust (Fig. 4b), according to the values of PDR (Fig. 4a). Figure 4c shows the final dust profile where, according to the flowchart in Fig. 3, the part between 4 and 7 km has been removed, because the total PBC is too small to be considered reliable, as well as the part above 7 km because there are cirrus clouds.

CONCLUSIONS

As product of the activity 4.11 a desert dust product will be released with the method here described. This will be applied to all the Italian datasets collected within ACTRIS/EARLINET satisfying the technical requirements in terms of collected variables and data quality. The data products, i.e. the vertical profiles of *Dust Backscatter Coefficient* and *Dust Extinction Coefficient*, will be securely stored and provided through the ITINERIS HUB (within WP2) and used in VRE AERO (WP8). At the present time, we expect to provide desert dust profiles for 5 aerosol lidar sites in Italy equipped with depolarization capability. The dataset will span, even if with different data coverage rate, the 2012-2024 period.

The data will be reported in netcdf (Annex 1 reports the designed data format) and will have the same main structure of the optical products provided by ACTRIS/EARLINET, adding new variables which are the dust backscatter and the dust extinction with its own statistical error. Reference to original ACTRIS/EARLINET data product will be reported for traceability and the code for processing ACTRIS/EARLINET data to obtain the dust product will be made available on github. Depending on the amount of data available for each station, it will be decided the specific granularity of each dataset (to which a DOI will be assigned). Additionally, a DOI will be associated to the whole collection of dust product.

REFERENCES

Ansmann, A., P. Seifert, M. Tesche, and U. Wandinger: Profiling of fine and coarse particle mass: case studies of Saharan dust and Eyjafjallajökull/Grimsvötn volcanic plumes. Atmos. Chem. Phys., 12, 9399–9415, doi:10.5194/acp-12-9399-2012, 2012.

Barnaba, F., Bolignano, A., Di Liberto, L., Morelli, M., Lucarelli, F., Nava, S., Perrino, C., Canepari, S., Basart, S., Costabile, F., Dionisi, D., Ciampichetti, S., Sozzi, R., Gobbi, G. P.: Desert dust contribution to PM10 loads in Italy: Methods and recommendations addressing the relevant European Commission Guidelines in support to the Air Quality Directive 2008/50, Atmos. Environ., 161, 288-305, https://doi.org/10.1016/j.atmosenv.2017.04.038, 2017.

Boselli, A., Caggiano, R., Cornacchia, C., Madonna, F., Macchiato, M., Mona, L., Pappalardo, G., and Trippetta, S.: Multi year sun-photometer measurements for aerosol characterization in a Central Mediterranean site, Atmos. Res., 104, 98-110, doi:10.1016/j.atmosres.2011.08.002, 2012.

Cordero, R.R., Damiani, A., Laroze, D. *et al.* Effects of soiling on photovoltaic (PV) modules in the Atacama Desert. *Sci Rep* **8**, 13943 (2018). https://doi.org/10.1038/s41598-018-32291-8

Di Mauro, B., Garzonio, R., Rossini, M., Filippa, G., Pogliotti, P., Galvagno, M., Morra di Cella, U., Migliavacca, M., Baccolo, G., Clemenza, M., Delmonte, B., Maggi, V., Dumont, M., Tuzet, F., Lafaysse, M., Morin, S., Cremonese, E., and Colombo, R.: Saharan dust events in the European Alps: role in snowmelt and geochemical characterization, The Cryosphere, 13, 1147–1165, https://doi.org/10.5194/tc-13-1147-2019, 2019.

Flaounas, E., Kotroni, V., Lagouvardos, K., Kazadzis, S., Gkikas, A., and Hatzianastassiou, N.: Cyclone contribution to dust transport over the Mediterranean region, Atmos. Sci. Lett., 16, 473–478, https://doi.org/10.1002/asl.584, 2015.

Freudenthaler, V., and Coauthors: Depolarization ratio profiling at several wavelengths in pure Saharan dust during SAMUM 2006. Tellus B, 61, 165–179, https://doi.org/10.1111/j.1600-0889.2008.00396.x, 2009.

Gkikas, A., Hatzianastassiou, N., Mihalopoulos, N., Katsoulis, V., Kazadzis, S., Pey, J., Querol, X., and Torres, O.: The regime of intense desert dust episodes in the Mediterranean based on contemporary satellite observations and ground measurements, Atmos. Chem. Phys., 13, 12135–12154, https://doi.org/10.5194/acp-13-12135-2013, 2013.

Gkikas, A., Houssos, E. E., Lolis, C. J., Bartzokas, A., Mihalopoulos, N., and Hatzianastassiou, N.: Atmospheric circulation evolution related to desert-dust episodes over the Mediterranean, Q. J. Roy. Meteor. Soc., 141, 1634–1645, https://doi.org/10.1002/qj.2466, 2015.

Gkikas, A., Basart, S., Hatzianastassiou, N., Marinou, E., Amiridis, V., Kazadzis, S., Pey, J., Querol, X., Jorba, O., Gassó, S., and Baldasano, J. M.: Mediterranean intense desert dust outbreaks and their vertical structure based on remote sensing data, Atmos. Chem. Phys., 16, 8609–8642, https://doi.org/10.5194/acp-16-8609-2016, 2016.

Gkikas, A., Proestakis, E., Amiridis, V., Kazadzis, S., Di Tomaso, E., Marinou, E., Hatzianastassiou, N., Kok, J. F., and García-Pando, C. P.: Quantification of the dust optical depth across spatiotemporal scales with the MIDAS global dataset (2003–2017), Atmos. Chem. Phys., 22, 3553–3578, https://doi.org/10.5194/acp-22-3553-2022, 2022.

Gupta P, Singh S, Kumar S, Choudhary M, Singh V. Effect of dust aerosol in patients with asthma. J Asthma. 2012 Mar;49(2):134-8. doi: 10.3109/02770903.2011.645180. Epub 2012 Jan 3. PMID: 22211448.

Kennedy, J., Lo, A., Rajamani, H-S. and Lutfi S.; Solar and sand: Dust deposit mitigation in the desert for PV arrays, Sustainable Energy, Grids and Networks, Vol. 28, 2021, https://doi.org/10.1016/j.segan.2021.100531

Mallone, S., Stafoggia, M., Faustini, A., Gobbi, G. P., Marconi, A., and Forastiere, F.: Saharan dust and associations between particulate matter and daily mortality in Rome, Italy, Environ. Health Persp., 119, 1409–1414, https://doi.org/10.1289/ehp.1003026, 2011.

Marenco, F., and R. J. Hogan: Determining the contribution of volcanic ash and boundary layer aerosol in backscatter lidar returns: A three-component atmosphere approach. J. Geophys Res., 116, D00U06, https://doi.org/10.1029/2010JD015415, 2011.

Meloni, D., di Sarra, A., Biavati, G., DeLuisi, J.J., Monteleone, F., Pace, G., Piacentino, S., and Sferlazzo, D.M., Seasonal behavior of Saharan dust events at the Mediterranean island of Lampedusa in the period 1999-2005, Atmospheric Environment, Vol.41, Issue 14, 2007, pp. 3041-3056, https://doi.org/10.1016/j.atmosenv.2006.12.001.

Mona, L., Amodeo, A., Pandolfi, M., and Pappalardo, G.: Saharan dust intrusions in the Mediterranean area: Three years of Raman lidar measurements, J. Geophys. Res.-Atmos., 111, D16203, https://doi.org/10.1029/2005JD006569, 2006.

Mona, L., Z. Liu, D. Müller, A. Omar, A. Papayannis, G. Pappalardo, N. Sugimoto, M. Vaughan, Lidar measurements for desert dust characterization: an Overview, Advances in Meteorology Advances in Meteorology, Volume 2012, Article ID 356265, 36 pages, doi:10.1155/2012/356265, http://www.hindawi.com/journals/amet/2012/356265/, 2012.

Mona, L., N. Papagiannopoulos, S. Basart, J. Baldasano, I. Binietoglou, C. Cornacchia, and G. Pappalardo, EARLINET dust observations vs. BSC-DREAM8b modeled profiles: 12-year-long systematic comparison at Potenza, Italy, Atmos. Chem. Phys., 14, 8781–8793, 2014, www.atmos-chem-phys.net/14/8781/2014/, doi:10.5194/acp-14-8781-2014, 2014.

Mona, L., and Coauthors, Observing Mineral Dust in Northern Africa, the Middle East, and Europe: Current Capabilities and Challenges ahead for the Development of Dust Services. Bull. Amer. Meteor. Soc., 104, E2223–E2264, https://doi.org/10.1175/BAMS-D-23-0005, 2023.

Monteiro, A., Basart, S., Kazadzis, S., Votzis, A., Gkikas, A., Vandenbussche, S., Tobias, A., Gama, C., García-Pando, C. P., Terradellas, E., Notas, G., Middleton, N., Kushta, J., Amiridis, V., Lagouvardos, K., Kosmopoulos, P., Kotroni, V., Kanakidou, M., Mihalopoulos, N., Kalivitis, N., Dagsson-Waldhauserová, P., El-Askary, H., Sievers, K., Giannaros, T., Mona, L., Hirtl, M., Skomorowski, P., Virtanen, T. H., Christoudias, T., Di Mauro, B., Trippetta, S., Kutuzov, S., Meinander, O., and Nickovic, S.: Multi-sectoral impact assessment of an extreme African dust episode in the Eastern Mediterranean in March 2018, Sci. Total Environ., 843, 156861, https://doi.org/10.1016/j.scitotenv.2022.156861, 2022.

Nogueira, J., Evangelista, H., Valeriano, C.d.M. et al. Dust arriving in the Amazon basin over the past 7,500 years came from diverse sources. Commun Earth Environ 2, 5 (2021). https://doi.org/10.1038/s43247-020-00071-w

Pace, G., di Sarra, A., Meloni, D., Piacentino, S., and Chamard, P.: Aerosol optical properties at Lampedusa (Central Mediterranean). 1. Influence of transport and identification of different aerosol types, Atmos. Chem. Phys., 6, 697–713, https://doi.org/10.5194/acp-6-697-2006, 2006.

Papagiannopoulos, N., Mona, L., Amodeo, A., D'Amico, G., Gumà Claramunt, P., Pappalardo, G., Alados-Arboledas, L., Guerrero-Rascado, J. L., Amiridis, V., Kokkalis, P., Apituley, A., Baars, H., Schwarz, A., Wandinger, U., Binietoglou, I., Nicolae, D., Bortoli, D., Comerón, A., Rodríguez-Gómez, A., Sicard, M., Papayannis, A., and Wiegner, M.: An automatic observation-

based aerosol typing method for EARLINET, Atmos. Chem. Phys., 18, 15879–15901, https://doi.org/10.5194/acp-18-15879-2018, 2018.

Schepanski, K., Heinold, B., and Tegen, I.: Harmattan, Saharan heat low, and West African monsoon circulation: modulations on the Saharan dust outflow towards the North Atlantic, Atmos. Chem. Phys., 17, 10223–10243, https://doi.org/10.5194/acp-17-10223-2017, 2017.

Shimizu, A., T. Nishizawa, J. Jin, S.-W. Kim, Z. Wang, D. Batdorj, and N. Sugimoto: Evolution of a lidar network for tropospheric aerosol detection in East Asia. Opt. Eng., 56(3), 031219, https://doi.org/10.1117/1.OE.56.3.031219, 2017.

Sugimoto, N., I. Uno, M. Nishikawa, A. Shimizu, I. Matsui, X. Dong, Y. Chen, and H. Quan: Record heavy Asian dust in Beijing in 2002: Observations and model analysis of recent events. Geophys. Res. Lett., 30, 1640, https://doi.org/10.1029/2002GL016349, 2003.

Tesche, M., Barnaba, A., Müller, D., Althausen, D., Engelmann, R., Freudenthaler, V., and Grob, S.: Vertically Resolved Separation of Dust and Smoke over Cape Verde Using Multiwavelength Raman and Polarization Lidars during Saharan Mineral Dust Experiment 2008, J. Geophys. Res., 114, D13202, doi:10.1029/2009JD011862, 2009.

UNCCD: Sand and Dust Storms Compendium: Information and Guidance on Assessing and Addressing the Risks, United Nations Convention to Combat Desertification, Bonn, Germany, https://www.unccd.int/resources/publications/sand-and-duststorms-compendium-information-and-guidance-assessing-and (last access: 13 January 2024), 2022.

Vergadi E, Rouva G, Angeli M, Galanakis E. Infectious Diseases Associated with Desert Dust Outbreaks: A Systematic Review. Int J Environ Res Public Health. 2022 Jun 5;19(11):6907. doi: 10.3390/ijerph19116907. PMID: 35682493; PMCID: PMC9180817.

WHO: WHO global air quality guidelines: particulate matter (PM2.5 and PM10), ozone, nitrogen dioxide, sulfur dioxide and carbon monoxide, World Health Organization, https://apps.who.int/iris/handle/10665/345329 (last access: 13 January 2024), 2021.

Yu, H., Tan, Q., Zhou, L., Zhou, Y., Bian, H., Chin, M., Ryder, C. L., Levy, R. C., Pradhan, Y., Shi, Y., Song, Q., Zhang, Z., Colarco, P. R., Kim, D., Remer, L. A., Yuan, T., Mayol-Bracero, O., and Holben, B. N.: Observation and modeling of the historic "Godzilla" African dust intrusion into the Caribbean Basin and the southern US in June 2020, Atmos. Chem. Phys., 21, 12359–12383, https://doi.org/10.5194/acp-21-12359-2021, 2021.

Yumimoto K., I. Uno, N. Sugimoto, A. Shimizu, Z. Liu, and D.M. Winker, 2008: Adjoint inversion modeling of Asian dust emission using lidar observations. Atmos. Chem. Phys., 8, 2869–2884, https://doi.org/10.5194/acp-8-2869-2008.

ANNEX 1 – DUST PRODUCT DATA EXAMPLE

```
netcdf Dust_Product_pot_Lev02_b0532_202109132130_202109132317_v01_qc03 {
dimensions:
        time = 1 ;
        wavelength = 1 ;
        altitude = 178 ;
        nv = 2 ;
variables:
        double time(time) ;
                time:axis = "T" ;
                time:bounds = "time_bounds" ;
                time:calendar = "gregorian" ;
                time:long_name = "time" ;
                time:standard_name = "time" ;
                time:units = "seconds since 1970-01-01T00:00:00Z" ;
        double time_bounds(time, nv) ;
        double altitude(altitude) ;
                altitude:axis = "Z" ;
                altitude:long_name = "height above sea level" ;
                altitude:positive = "up" ;
                altitude:standard_name = "altitude" ;
                altitude:units = "m" ;
        float wavelength(wavelength) ;
                wavelength:long_name = "wavelength of the transmitted laser pulse" ;
                wavelength:units = "nm" ;
        byte error_retrieval_method(wavelength) ;
                error_retrieval_method:long_name = "method used for the retrieval of
uncertainties" ;
                error_retrieval_method:_FillValue = -127b ;
                error_retrieval_method:flag_values = 0b, 1b ;
                error_retrieval_method:flag_meanings = "monte_carlo
error_propagation" ;
        byte backscatter_evaluation_method(wavelength) ;
                backscatter_evaluation_method:long_name = "method used for the
backscatter retrieval" ;
                backscatter_evaluation_method:_FillValue = -127b ;
                backscatter_evaluation_method:flag_values = 0b, 1b ;
                backscatter_evaluation_method:flag_meanings = "Raman
elastic_backscatter" ;
        float longitude ;
                longitude:long_name = "longitude of station" ;
                longitude:standard_name = "longitude" ;
                longitude:units = "degrees_east" ;
        float latitude ;
                latitude:long_name = "latitude of station" ;
                latitude:standard_name = "latitude" ;
```

```
                latitude:units = "degrees_north" ;
        float station_altitude ;
                station_altitude:long_name = "station altitude above see level" ;
                station_altitude:units = "m" ;
                station_altitude:_FillValue = 9.96921e+36f ;
        float zenith_angle ;
                zenith_angle:long_name = "laser pointing angle with respect to the
zenith" ;
                zenith_angle:units = "degrees" ;
                zenith_angle:_FillValue = 9.96921e+36f ;
        int shots(time) ;
                shots:long_name = "accumulated laser shots" ;
                shots:units = "1" ;
                shots:_FillValue = -2147483647 ;

double backscatter(wavelength, time, altitude) ;
                backscatter:ancillary_variables = "error_backscatter vertical_resolution" ;
                backscatter:coordinates = "longitude latitude" ;
                backscatter:long_name = "aerosol backscatter coefficient" ;
                backscatter:plausibility = "parameter passed the EARLINET quality
assurance." ;
                backscatter:units = "m-1*sr-1" ;
                backscatter:_FillValue = 9.96920996838687e+36 ;
        double error_backscatter(wavelength, time, altitude) ;
                error_backscatter:coordinates = "longitude latitude" ;
                error_backscatter:long_name = "statistical uncertainty of aerosol
backscatter" ;
                error_backscatter:plausibility = "parameter passed the EARLINET
quality assurance." ;
                error_backscatter:units = "m-1*sr-1" ;
                error_backscatter:_FillValue = 9.96920996838687e+36 ;
double vertical_resolution(wavelength, time, altitude) ;
                vertical_resolution:long_name = "effective vertical resolution according
to Pappalardo et al., appl. opt. 2004" ;
                vertical_resolution:units = "m" ;
                vertical_resolution:_FillValue = 9.96920996838687e+36 ;

double particledepolarization(wavelength, time, altitude) ;
                particledepolarization:coordinates = "longitude latitude" ;
                particledepolarization:long_name = "aerosol linear depolarization ratio" ;
                particledepolarization:plausibility = "parameter not quality assured by
EARLINET." ;
                particledepolarization:units = "1" ;
                particledepolarization:_FillValue = 9.96920996838687e+36 ;
        double error_particledepolarization(wavelength, time, altitude) ;
                error_particledepolarization:coordinates = "longitude latitude" ;
                error_particledepolarization:long_name = "statistical uncertainty of
aerosol linear depolarization ratio" ;
```

error_particledepolarization:plausibility = "parameter not quality assured by EARLINET." ;
error_particledepolarization:units = "1" ;
error_particledepolarization:_FillValue = 9.96920996838687e+36 ;

byte cloud_mask_type ;
cloud_mask_type:long_name = "cloud mask type" ;
cloud_mask_type:_FillValue = -127b ;
cloud_mask_type:valid_range = 0b, 3b ;
cloud_mask_type:flag_values = 0b, 1b, 2b ;
cloud_mask_type:flag_meanings = "no_cloudmask_available manual_cloudmask automatic_cloudmask" ;
byte scc_product_type ;
scc_product_type:long_name = "SCC product type" ;
scc_product_type:_FillValue = -127b ;
scc_product_type:valid_range = 1b, 2b ;
scc_product_type:flag_values = 1b, 2b ;
scc_product_type:flag_meanings = "experimental operational" ;
byte cloud_mask(time, altitude) ;
cloud_mask:long_name = "cloud mask" ;
cloud_mask:_FillValue = -127b ;
cloud_mask:valid_range = 0b, 7b ;
cloud_mask:flag_masks = 1b, 2b, 4b ;
cloud_mask:flag_meanings = "unknown_cloud cirrus_cloud water_cloud" ;

double dust_backscatter(wavelength, time, altitude) ;
dust_backscatter:ancillary_variables = "error_dust_backscatter vertical_resolution" ;
dust_backscatter:coordinates = "longitude latitude" ;
dust_backscatter:long_name = "dust backscatter coefficient" ;

dust_backscatter:units = "m-1*sr-1" ;
dust_backscatter:_FillValue = 9.96920996838687e+36 ;

double error_dust_backscatter(wavelength, time, altitude) ;
error_dust_backscatter:coordinates = "longitude latitude" ;
error_dust_backscatter:long_name = "statistical uncertainty of dust backscatter" ;
error_dust_backscatter:plausibility = " parameter not quality assured by EARLINET." ;
error_dust_backscatter:units = "m-1*sr-1" ;
error_dust_backscatter:_FillValue = 9.96920996838687e+36 ;
double vertical_resolution(wavelength, time, altitude) ;
vertical_resolution:long_name = "effective vertical resolution according to Pappalardo et al., appl. opt. 2004" ;

vertical_resolution:units = "m" ;
vertical_resolution:_FillValue = 9.96920996838687e+36 ;

double dust_extinction(wavelength, time, altitude) ;
dust_ extinction:ancillary_variables = "error_dust_ extinction vertical_resolution" ;
dust_ extinction:coordinates = "longitude latitude" ;
dust_ extinction:long_name = "dust extinction coefficient" ;

dust_ extinction:units = "m-1" ;
dust_ extinction:_FillValue = 9.96920996838687e+36 ;

double error_dust_ extinction (wavelength, time, altitude) ;
error_dust_ extinction:coordinates = "longitude latitude" ;
error_dust_ extinction:long_name = "statistical uncertainty of dust extinction " ;
error_dust_ extinction:plausibility = " parameter not quality assured by EARLINET." ;
error_dust_ extinction:units = "m-1" ;
error_dust_ extinction:_FillValue = 9.96920996838687e+36 ;
double vertical_resolution(wavelength, time, altitude) ;
vertical_resolution:long_name = "effective vertical resolution according to Pappalardo et al., appl. opt. 2004" ;
vertical_resolution:units = "m" ;
vertical_resolution:_FillValue = 9.96920996838687e+36 ;

// global attributes:
:Conventions = "CF-1.7" ;
:title = "Profiles of aerosol optical properties" ;
:source = "Ground based LIDAR measurements" ;
:references = "Dust product obtained using ACTRIS/EARLINET data and Tesche et al., 2009 method" ;
:history = "Created on 2022-02-27T00:10Z " ;
:station_ID = "pot" ;
:location = "Potenza, Italy" ;
:system = "MUSA" ;
:institution = "Consiglio Nazionale delle Ricerche - Istituto di Metodologie per l\'Analisi Ambientale (CNR-IMAA), Potenza - CNR-IMAA" ;
:comment = "" ;
:measurement_ID = "20210913pot2130" ;
:measurement_start_datetime = "2021-09-13T21:30:25Z" ;
:measurement_stop_datetime = "2021-09-13T23:17:21Z" ;
:PI = "Aldo Amodeo" ;
:PI_affiliation = "Consiglio Nazionale delle Ricerche - Istituto di Metodologie per l\'Analisi Ambientale " ;
:PI_affiliation_acronym = "CNR-IMAA" ;

:PI_address = "Contrada S.Loja, Zona Industriale - Tito Scalo I-85050 Potenza" ;
:PI_phone = "+39 0971 427263" ;
:PI_email = "aldo.amodeo@imaa.cnr.it" ;
:Data_Originator = "pot_uploader" ;
:Data_Originator_affiliation = "Consiglio Nazionale delle Ricerche - Istituto di Metodologie per l\'Analisi Ambientale" ;
:Data_Originator_affiliation_acronym = "CNR-IMAA" ;
:Data_Originator_address = "Contrada S.Loja, Zona Industriale - Tito Scalo I-85050 Potenza" ;
:Data_Originator_phone = "+39 0971 427263" ;
:Data_Originator_email = "aldo.amodeo@imaa.cnr.it" ;
:data_processing_institution = "Consiglio Nazionale delle Ricerche - Istituto di Metodologie per l\'Analisi Ambientale (CNR-IMAA)" ;
:hoi_system_ID = 74 ;
:hoi_configuration_ID = 559 ;
:processor_name=”DustProfiler”;
:processor_version = "1.0" ;

:input_file = " EARLINET_AerRemSen_pot_Lev02_b0532_202109132130_202109132317_v02_qc03.nc " ;

:__acknowledgments: “The activities leading to this data product were funded by ITINERIS (Italian Integrated Environmental Research Infrastructures System)”, PNRR, Project code IR0000032

data:

time = 1631568625; // time(1)

time_bounds =
1631568625, // time_bounds(1,1)
1631575041; // time_bounds(2,1)

altitude = 1030, // altitude(1)
…..
11650; // altitude(178)

wavelength = 532; // wavelength(1)

error_retrieval_method = 1; // error_retrieval_method(1)

backscatter_evaluation_method = 0; // backscatter_evaluation_method(1)

raman_backscatter_algorithm = 1; // raman_backscatter_algorithm(1)

longitude = 15.72; // longitude(1145785199)

latitude = 40.6; // latitude(1147882255)

station_altitude = 760; // station_altitude(1148275461)

zenith_angle = 0; // zenith_angle(1144736639)

shots = 3672000; // shots(1)

atmospheric_molecular_calculation_source = 2; // atmospheric_molecular_calculation_source(1145129845)

cirrus_contamination = 2; // cirrus_contamination(1145391985)

cirrus_contamination_source = 2; // cirrus_contamination_source(1144998779)

quality_control_level = 2; // quality_control_level(1146309479)

basic_quality_control = 7; // basic_quality_control(1147095835)

advanced_quality_control = 2027; // advanced_quality_control(1145981802)

backscatter =
 1.89244926570046e-06, // backscatter(1,1,1)
…..
  9.39888494713363e-08; // backscatter(178,1,1)

error_backscatter =
 4.59075292690807e-08, // error_backscatter(1,1,1)
….
  9.05585864288758e-08; // error_backscatter(178,1,1)

vertical_resolution =
 180, // vertical_resolution(1,1,1)
……
  540; // vertical_resolution(178,1,1)

particledepolarization =
 0.046053690950082, // particledepolarization(1,1,1)
….
  _; // particledepolarization(178,1,1)

error_particledepolarization =
 0.000588184273299376, // error_particledepolarization(1,1,1)
…

```
   _;  // error_particledepolarization(178,1,1)

dust_backscatter =
  1.89244926570046e-06,   // dust_backscatter(1,1,1)
…..
   9.39888494713363e-08;  // dust_backscatter(178,1,1)

 error_dust_backscatter =
  4.59075292690807e-08,   // error_dust_backscatter(1,1,1)
….
   9.05585864288758e-08;  // error_dust_backscatter(178,1,1)
dust_extinction =
  1.89244926570046e-04,   // dust_ extinction (1,1,1)
…..
   9.39888494713363e-06;  // dust_ extinction (178,1,1)

 error_dust_ extinction =
  4.59075292690807e-05,   // error_dust_ extinction (1,1,1)
….
   9.05585864288758e-07;  // error_dust_ extinction (178,1,1)




 cloud_mask_type = 2;  // cloud_mask_type(1145129845)


 cloud_mask =
  0,   // cloud_mask(1,1)
….
   0;  // cloud_mask(178,1)
   }
```